

# Epitope Mapping of the Anti-CD44 Monoclonal Antibody (C<sub>44</sub>Mab-46) Using Alanine-Scanning Mutagenesis and Surface Plasmon Resonance

Junko Takeji,<sup>1,\*</sup> Teizo Asano,<sup>1,\*</sup> Hiroyuki Suzuki,<sup>2</sup> Mika K. Kaneko,<sup>1</sup> and Yukinari Kato<sup>1,2,i</sup>

CD44 is a type I transmembrane protein expressed in various kinds of normal cancer cells, including pancreatic, breast, and oral cancers. CD44 is associated with cancer progression, metastases, and treatment resistance. CD44 consists of 20 exons, and various isoforms exist due to alternative splicing of the central 10 exons. Some splicing variants show cancer-specific expression patterns and are related to prognosis of patients with cancer. Therefore, CD44 targeting therapy has been attracting attention. In a previous study, we established an anti-CD44 monoclonal antibody, C<sub>44</sub>Mab-46 (IgG<sub>1</sub>, kappa), useful for flow cytometry, Western blotting, and immunohistochemistry by immunizing mice with CD44v3-10 ectodomain. This study investigated the binding epitope of C<sub>44</sub>Mab-46 using enzyme-linked immunosorbent assay (ELISA) and the surface plasmon resonance (SPR) with the synthesized peptide. ELISA results using deletion mutants showed that C<sub>44</sub>Mab-46 reacted with the amino acids (aa) of 161–180 aa of CD44. Further examination of the C<sub>44</sub>Mab-46 epitope using ELISA with point mutants in 161–180 aa of CD44 demonstrates that the C<sub>44</sub>Mab-46 epitope comprised Thr174, Asp177, and Val178. The SPR with point mutants in 161–180 aa of CD44 demonstrated that the C<sub>44</sub>Mab-46 epitope comprises Thr174, Asp175, Asp176, Asp177, and Val178. Together, the C<sub>44</sub>Mab-46 epitope was determined to be located in exon 5 of CD44.

**Keywords:** CD44, monoclonal antibody, epitope mapping, surface plasmon resonance

## Introduction

CD44 is a single span transmembrane glycoprotein with various functions, such as cell adhesion, growth, survival, differentiation, and motility.<sup>(1)</sup> The principal ligand of CD44 is hyaluronic acid (HA), osteopontin, serglycin, collagens, fibronectin, and laminin also bind with CD44.<sup>(2)</sup> The full-length CD44 gene consists of 20 exons. The standard isoform (CD44s) consists of exons 1–5 and 16–20, which are expressed in all isoforms. The other exons are alternatively spliced to generate splicing variants (CD44v). The predicted molecular mass of CD44s is 37–38 kDa, and post-translational modifications, including *N*- and *O*-linked glycosylation, sulfation, and phosphorylation increase the molecular mass to 85–95 kDa. The largest possible molecular mass of CD44 is >200 kDa.<sup>(3)</sup>

CD44 is expressed in various tissues, such as the central nervous system, lung, epidermis, liver, and pancreas.<sup>(4)</sup> CD44 expression is also observed in many cancers, including pancreatic cancer,<sup>(5)</sup> breast cancer,<sup>(6)</sup> lung cancer,<sup>(7)</sup> gastric

cancer,<sup>(8)</sup> colorectal cancer,<sup>(9)</sup> and head and neck squamous cell carcinoma (HNSCC).<sup>(10)</sup> Günthert et al. found CD44 variant isoforms, which contains exons v4–v7 from rat pancreatic carcinoma cell line, and its overexpression converted the nonmetastatic cells into metastatic cells.<sup>(11)</sup> Further study revealed that an anti-CD44v6 monoclonal antibody (mAb) prevented the metastatic property of these cells.<sup>(12)</sup> CD44v6-bearing isoforms play an essential role in metastases by promoting c-Met activation.<sup>(13)</sup> HA binding to CD44 affects tumor development by inhibiting apoptosis and promoting invasion and angiogenesis.<sup>(14)</sup> CD44 also interacts with epidermal growth factor receptor (EGFR) and human epidermal growth factor receptor 2.<sup>(15–17)</sup> The HA/CD44 interaction leads to CD44-EGFR complex formation, and the complex induces downstream signaling through Ras and RhoA, resulting in tumor cell growth. HA/CD44 signaling also leads to increased cisplatin chemoresistance through EGFR signaling pathways in HNSCC.<sup>(10)</sup> In these ways, CD44 activates and modulates several cell signals that mediate tumor progression, metastasis, and therapy resistance.

Departments of <sup>1</sup>Antibody Drug Development, and <sup>2</sup>Molecular Pharmacology, Tohoku University Graduate School of Medicine, Sendai, Japan.

\*Contributed equally to this study.

<sup>i</sup>ORCID ID (<https://orcid.org/0000-0001-5385-8201>).

Head and neck cancer (HNC) are the seventh most common cancer worldwide in 2020. About 930,000 people are newly diagnosed with HNC, and 470,000 people have died of it.<sup>(18)</sup> More than 90% of cases are pathologically diagnosed with squamous cell carcinoma.<sup>(19)</sup> Some antibody drugs for HNSCC have been approved: cetuximab, an anti-EGFR mAb, was first approved in 2006,<sup>(20)</sup> and later, nivolumab and pembrolizumab, which are anti-PD-1 mAbs, were approved in 2016.<sup>(21)</sup> These drugs have improved the prognoses of patients with HNSCC; however, they have some problems. Adverse effects such as skin toxicity and interstitial lung disease are observed in cetuximab,<sup>(22,23)</sup> and patients with PD-L1 negative receive little benefits.<sup>(24)</sup> Acquired resistance is also found in all drugs. Therefore, other therapeutic targets are needed.

In HNSCC, it was reported that some CD44-splicing variants such as CD44v3, v4, v6, and v10 were expressed in addition to CD44s.<sup>(25,26)</sup> Wang et al. reported that their expression was associated with advanced T stage (v3 and v6), metastasis (v3 and v10), and shorter disease-free survival (v6 and v10).<sup>(26)</sup> Previously, bivatuzumab mertansine, an anti-CD44v6 mAb linked to a cytotoxic drug, was used in phase I trial; however, it was discontinued because of severe skin toxicity with a fatal outcome in parallel trial.<sup>(27)</sup> Therefore, the development of other anti-CD44 targeting drugs that have fewer side effects is desired.

We previously developed an anti-CD44 mAbs, C<sub>44</sub>Mab-46 (IgG<sub>1</sub>, kappa), by immunizing mice with CD44v3-10 ectodomain. This study investigated its critical epitopes using enzyme-linked immunosorbent assay (ELISA) and surface plasmon resonance (SPR) with synthesized peptides.

## Materials and Methods

### Cell lines

A glioblastoma cell line (LN229) was obtained from the American Type Culture Collection (Manassas, VA). CD44v3-10 ectodomain (CD44ec)-secreting LN229 (LN229/CD44ec) was established by transfecting pCAG/PA-CD44ec-RAP-MAP into LN229 cells using the Neon transfection system (Thermo Fisher Scientific, Inc., Waltham, MA). The amino acid (aa) sequences of the tag system in this study were as follows: PA tag,<sup>(28)</sup> 12 aa (GVAMPGAEDDVV); RAP tag,<sup>(29)</sup> 12 aa (DMVNPGLIEDRIE); and MAP tag,<sup>(30)</sup> 12 aa (GDGMVPPGIEDK). LN229 and LN229/CD44ec were cultured in Dulbecco's modified Eagle's medium (DMEM) complete medium, including DMEM (4.5 g/L glucose) with L-Gln and without sodium pyruvate (cat. no: 08459-64; Nacalai Tesque, Inc., Kyoto, Japan), 10% heat-inactivated fetal bovine serum (Thermo Fisher Scientific, Inc.), 100 U/mL of penicillin (Nacalai Tesque, Inc.), 100 µg/mL streptomycin (Nacalai Tesque, Inc.), and 0.25 µg/mL amphotericin B (Nacalai Tesque, Inc.). LN229/CD44ec was established in DMEM complete medium, including 0.5 mg/mL of G418 (Nacalai Tesque, Inc.). Cell lines were incubated at 37°C in a humid atmosphere containing 5% CO<sub>2</sub>.

### Purification of CD44ec

After LN229/CD44ec was cultured using DMEM complete medium without G418, CD44ec was purified from the supernatants using RAP tag system, comprised an anti-RAP tag mAb (clone PMab-2) and a RAP peptide

TABLE 1. IDENTIFICATION OF C<sub>44</sub>MAB-46 EPTOPE USING POINT MUTANTS BY ENZYME-LINKED IMMUNOSORBENT ASSAY

| Mutant peptide | Sequence              | C <sub>44</sub> Mab-46 |
|----------------|-----------------------|------------------------|
| Y161A          | ARTNPEDIYPSNPTDDDDVSS | +++                    |
| R162A          | YATNPEDIYPSNPTDDDDVSS | +++                    |
| T163A          | YRANPEDIYPSNPTDDDDVSS | +++                    |
| N164A          | YRTAPEDIYPSNPTDDDDVSS | +++                    |
| P165A          | YRTNAEDIYPSNPTDDDDVSS | +++                    |
| E166A          | YRTNPADIYPSNPTDDDDVSS | +++                    |
| D167A          | YRTNPEAIYPSNPTDDDDVSS | +++                    |
| I168A          | YRTNPEDAYPSNPTDDDDVSS | +++                    |
| Y169A          | YRTNPEDIAPSNPTDDDDVSS | +++                    |
| P170A          | YRTNPEDIYASNPTDDDDVSS | +++                    |
| S171A          | YRTNPEDIYPANPTDDDDVSS | +++                    |
| N172A          | YRTNPEDIYSPATDDDDVSS  | +++                    |
| P173A          | YRTNPEDIYPSNATDDDDVSS | +++                    |
| T174A          | YRTNPEDIYPSNPADDDVSS  | +++                    |
| D175A          | YRTNPEDIYPSNPTADDVSS  | -                      |
| D176A          | YRTNPEDIYPSNPTDADVSS  | +++                    |
| D177A          | YRTNPEDIYPSNPTDDAVSS  | ++                     |
| V178A          | YRTNPEDIYPSNPTDDDVSS  | +                      |
| S179A          | YRTNPEDIYPSNPTDDDVAS  | +++                    |
| S180A          | YRTNPEDIYPSNPTDDDVSA  | +++                    |

+++; OD655 ≥ 0.5; ++, 0.3 ≤ OD655 < 0.5; +, 0.1 ≤ OD655 < 0.3; -, OD655 < 0.1.

(GDDMVNPGLIEDRIE).<sup>(29)</sup> The filtered culture supernatant (5 L) was passed through PMab-2-Sepharose (2 mL bed volume), and the same process was repeated three times. The beads were then washed with 100 mL of phosphate-buffered saline (PBS; Nacalai Tesque, Inc.), and eluted with 0.1 mg/mL a RAP peptide in a stepwise manner (2 mL × 10).

TABLE 2. THE K<sub>D</sub> BETWEEN C<sub>44</sub>MAB-46 AND ALANINE SUBSTITUTED PEPTIDES BY SURFACE PLASMON RESONANCE

| Mutant peptide | k <sub>a</sub> (/ms)   | k <sub>d</sub> (/s)     | K <sub>D</sub> (M)      |
|----------------|------------------------|-------------------------|-------------------------|
| p161-180       | 1.07 × 10 <sup>3</sup> | 6.32 × 10 <sup>-3</sup> | 5.92 × 10 <sup>-6</sup> |
| Y161A          | 1.06 × 10 <sup>3</sup> | 6.86 × 10 <sup>-3</sup> | 6.50 × 10 <sup>-6</sup> |
| R162A          | 1.29 × 10 <sup>3</sup> | 6.07 × 10 <sup>-3</sup> | 4.72 × 10 <sup>-6</sup> |
| T163A          | 1.30 × 10 <sup>3</sup> | 6.18 × 10 <sup>-3</sup> | 4.76 × 10 <sup>-6</sup> |
| N164A          | 2.22 × 10 <sup>3</sup> | 7.03 × 10 <sup>-3</sup> | 3.16 × 10 <sup>-6</sup> |
| P165A          | 1.39 × 10 <sup>3</sup> | 6.48 × 10 <sup>-3</sup> | 4.68 × 10 <sup>-6</sup> |
| E166A          | 1.51 × 10 <sup>3</sup> | 5.23 × 10 <sup>-3</sup> | 3.46 × 10 <sup>-6</sup> |
| D167A          | 1.70 × 10 <sup>3</sup> | 6.39 × 10 <sup>-3</sup> | 3.76 × 10 <sup>-6</sup> |
| I168A          | 1.22 × 10 <sup>3</sup> | 5.97 × 10 <sup>-3</sup> | 4.88 × 10 <sup>-6</sup> |
| Y169A          | 1.08 × 10 <sup>3</sup> | 6.16 × 10 <sup>-3</sup> | 5.70 × 10 <sup>-6</sup> |
| P170A          | 1.31 × 10 <sup>3</sup> | 6.82 × 10 <sup>-3</sup> | 5.20 × 10 <sup>-6</sup> |
| S171A          | 1.33 × 10 <sup>3</sup> | 5.08 × 10 <sup>-3</sup> | 3.81 × 10 <sup>-6</sup> |
| N172A          | 1.13 × 10 <sup>3</sup> | 4.72 × 10 <sup>-3</sup> | 4.16 × 10 <sup>-6</sup> |
| P173A          | 1.17 × 10 <sup>3</sup> | 1.72 × 10 <sup>-2</sup> | 1.47 × 10 <sup>-5</sup> |
| T174A          | ND                     | ND                      | 5.46 × 10 <sup>-5</sup> |
| D175A          | ND                     | ND                      | 4.75 × 10 <sup>-4</sup> |
| D176A          | ND                     | ND                      | 1.35 × 10 <sup>-4</sup> |
| D177A          | ND                     | ND                      | 1.33 × 10 <sup>-4</sup> |
| V178A          | ND                     | ND                      | 2.00 × 10 <sup>-4</sup> |
| S179A          | 1.30 × 10 <sup>3</sup> | 4.32 × 10 <sup>-3</sup> | 3.34 × 10 <sup>-6</sup> |
| S180A          | 1.21 × 10 <sup>3</sup> | 7.44 × 10 <sup>-3</sup> | 6.16 × 10 <sup>-6</sup> |

ND, not determined.

*CD44 peptides*

CD44 peptides (accession no. X66733), including 58 deletion mutants and 20 point mutants (Table 1), were synthesized using PEPscreen (Sigma-Aldrich Corp., St. Louis, MO).

*Enzyme-linked immunosorbent assay*

CD44ec and synthesized CD44 peptides (Table 1) were immobilized on Nunc Maxisorp 96-well immunoplates

(Thermo Fisher Scientific, Inc.) at a concentration of 1 and 10  $\mu\text{g/mL}$ , respectively, for 30 min at 37°C. After washing with PBS containing 0.05% Tween20 (Nacalai Tesque, Inc.; PBST), wells were blocked with 1% bovine serum albumin-containing PBST for 30 min at 37°C. The plates were incubated with C<sub>44</sub>Mab-46 (1  $\mu\text{g/mL}$ ), followed by a peroxidase-conjugated anti-mouse immunoglobulins (1:2000 diluted; Agilent Technologies, Inc., Santa Clara, CA). Enzymatic reactions were conducted by the ELISA POD

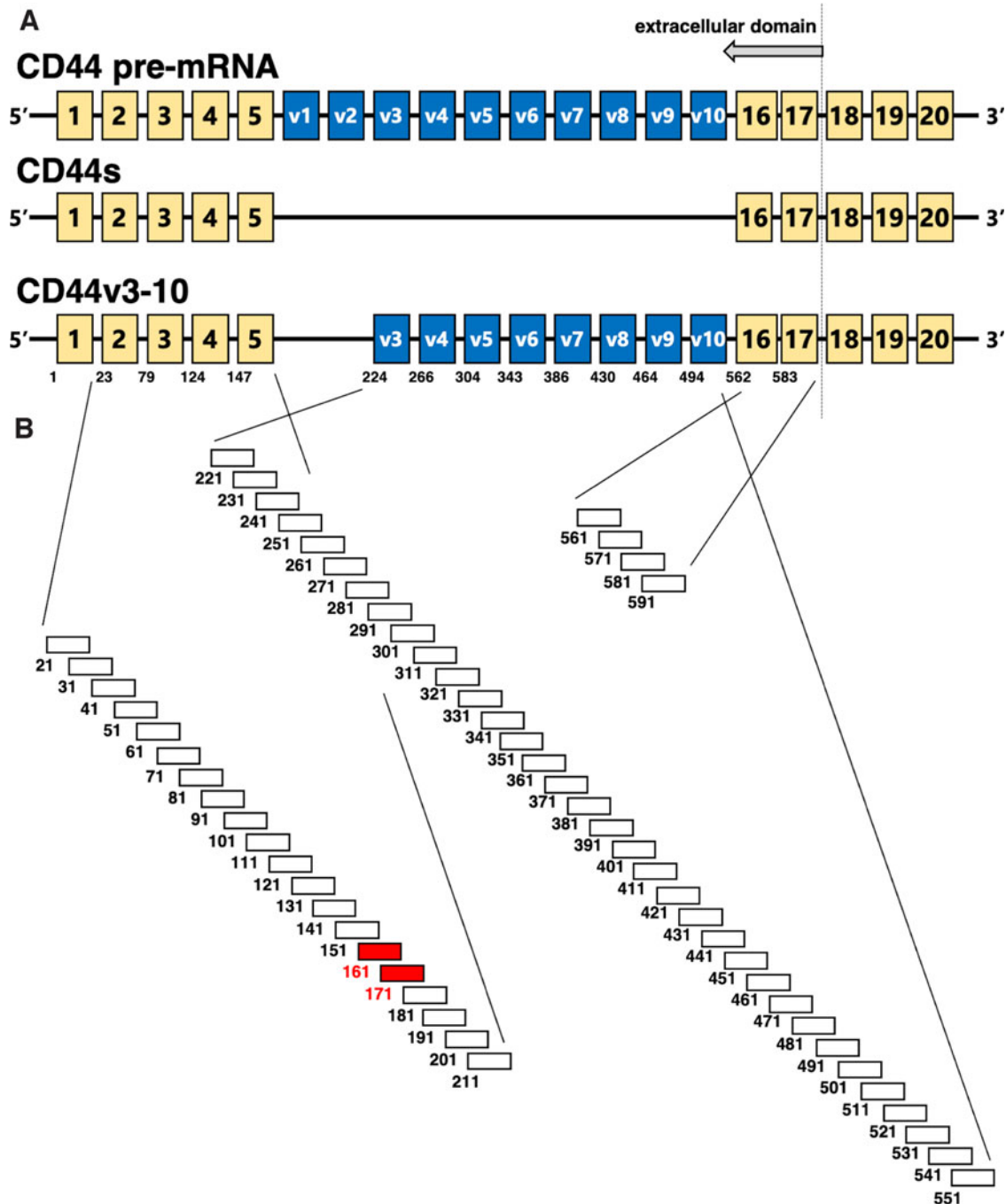


**FIG. 1.** (A) Schematic illustration of CD44 gene. The full-length CD44 gene consists of 20 exons (*upper panel*). The standard isoform (CD44s) consists of exons 1–5 and 16–20 (*middle panel*). The other exons are alternatively spliced to generate splicing variants, such as CD44v3-10, which consists of exons 1–5, v3–v10, and 16–20 (*lower panel*). (B) Schematic illustration of synthesized peptides. Red bars indicate the peptide detected by C<sub>44</sub>Mab-46.

Substrate TMB Kit (Nacalai Tesque, Inc.). Optical density was measured at 655 nm using an iMark microplate reader (Bio-Rad Laboratories, Inc., Berkeley, CA).

*Measurement of dissociation constants ( $K_D$ ) between C<sub>44</sub>Mab-46 and alanine-substituted peptides using SPR*

C<sub>44</sub>Mab-46 was immobilized on the sensor chip CM5 according to the protocol (<https://doi.org/10.1039/C39900001526>), described by Cytiva (Marlborough, MA). In brief, C<sub>44</sub>Mab-46 was diluted to 10  $\mu\text{g}/\text{mL}$  by the acetate buffer (pH 4.0; Cytiva) and immobilized using amine coupling reaction. The surface of the flow cell 2 of the sensor chip CM5 was treated with 1-ethyl-3-(3-dimethylaminopropyl)-carbodiimide and *N*-hydroxysuccinimide (NHS), followed by the injection of C<sub>44</sub>Mab-46. Unreacted NHS-ester was blocked with ethanolamine after C<sub>44</sub>Mab-46 immobilization. The  $K_D$  between C<sub>44</sub>Mab-46 and alanine-substituted peptides shown in Table 2 were measured using Biacore X100 (Cytiva) at 25°C. The buffer used was PBS containing 0.005% (v/v) of Tween 20 and 1.1% or 4.4% (v/v) of dimethyl sulfoxide (FUJIFILM Wako Pure Chemical Corporation, Osaka, Japan). A single cycle kinetics method was used to measure the binding signals. The data were analyzed by 1:1 binding kinetics to determine the association rate constant ( $k_a$ ) and dissociation rate constant ( $k_d$ ) and  $K_D$ , or equilibrium analysis to determine  $K_D$  using BIAevaluation software (Cytiva).

## Results

### Epitope mapping using ELISA

Fifty-eight peptides were synthesized (20 aa) from the extracellular domain of CD44v3-10 (Fig. 1) and performed ELISA. C<sub>44</sub>Mab-46 reacted with 161–180 aa (<sub>161</sub>-YRTNPEDIYPSNPTDDDDVSS<sub>-180</sub>) and 171–190 aa (<sub>171</sub>-SNPTDDDDVSSGSSSERSSTS<sub>-190</sub>) (Fig. 2). Because the reaction of C<sub>44</sub>Mab-46 to 161–180 aa is higher than that of 171–190 aa, we used 161–180 aa for alanine scanning.

A series of point mutants of 161–180 aa were synthesized (Table 1). C<sub>44</sub>Mab-46 strongly reacted with Y161A, R162A, T163A, N164A, P165A, E166A, D167A, I168A, Y169A, P170A, S171A, N172A, P173A, T174A, D176A, S179A, S180A, wild type 161–180 aa, and moderately reacted with D177A and V178A, but not with D175A (Fig. 3A). The results indicate that Asp175, Asp177, and Val178 are included in the critical epitopes of C<sub>44</sub>Mab-46 (Fig. 3B).

### Epitope mapping using SPR

We measured the  $K_D$  between C<sub>44</sub>Mab-46 and a series of point mutants of CD44 synthesized peptides (Table 1) using Biacore X100. The measured values are summarized in Table 2. The association rate constant ( $k_a$ ) and dissociation rate constant ( $k_d$ ) of T174A, D175A, D176A, D177A, and V178A were not determined; therefore, their  $K_D$ s were calculated using equilibrium analyses. The binding affinities of T174A, D175A, D176A, D177A, and V178A to C<sub>44</sub>Mab-46 were 9.2-, 80-, 22.8-,

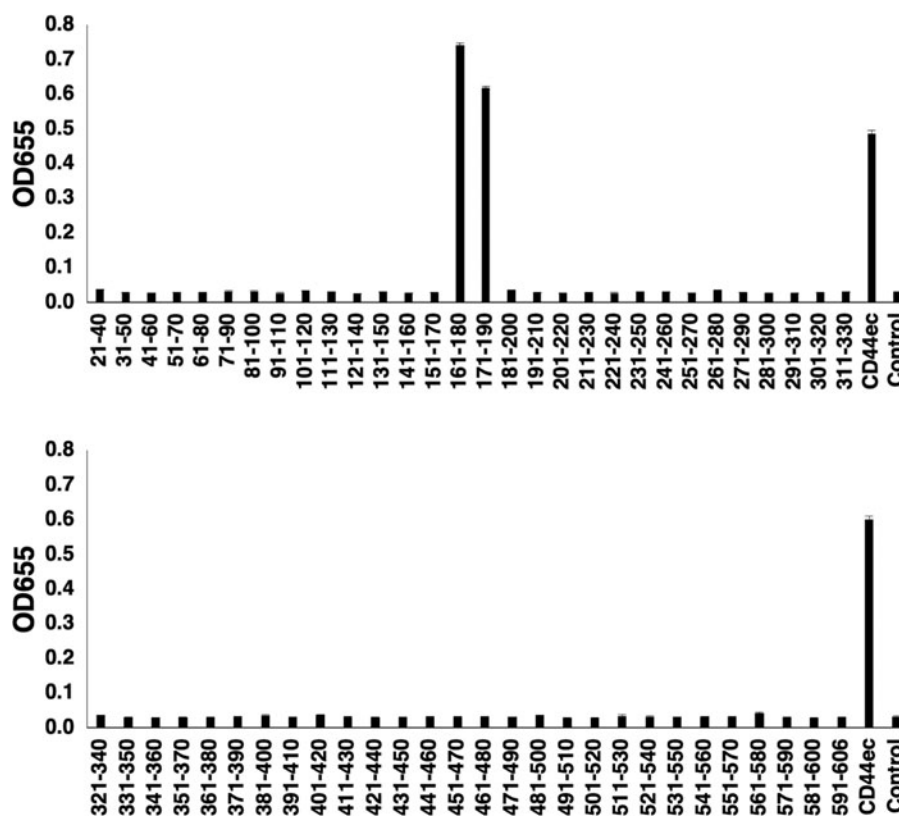


**FIG. 2.** Determination of C<sub>44</sub>Mab-46 epitope of CD44v3-10 by ELISA using deletion mutants. CD44ec (positive control), PBS (negative control), and synthesized peptides were immobilized on immunoplates. The plates were incubated with C<sub>44</sub>Mab-46 (1  $\mu\text{g}/\text{mL}$ ), followed by incubation with peroxidase-conjugated anti-mouse immunoglobulins. Optical density was measured at 655 nm. ELISA, enzyme-linked immunosorbent assay; PBS, phosphate-buffered saline.

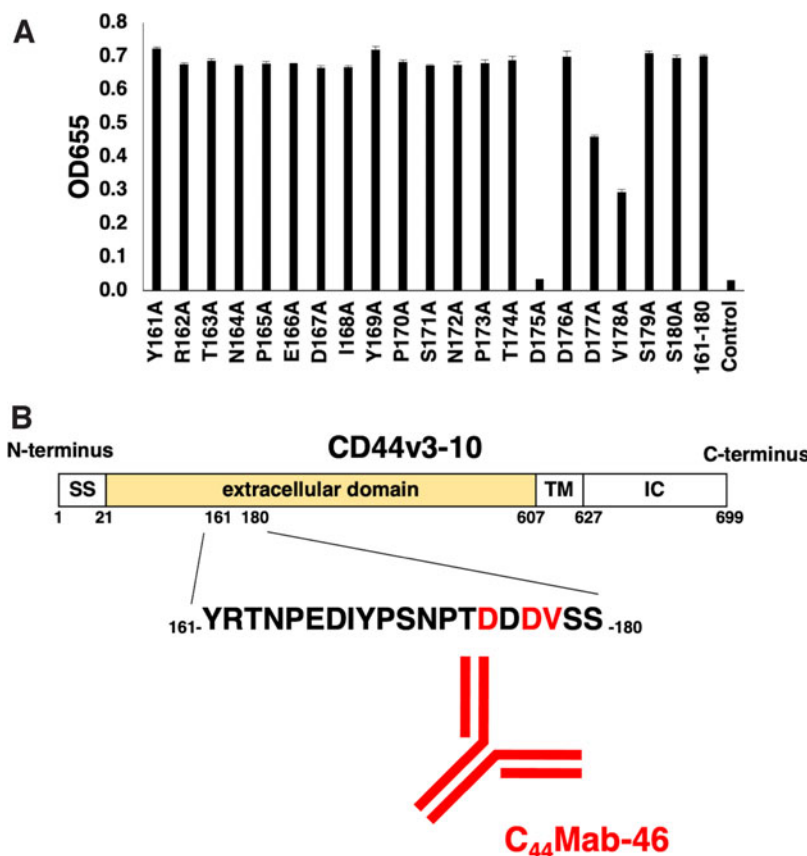


**FIG. 3.** (A) Determination of C<sub>44</sub>Mab-46 epitope of CD44v3-10 by ELISA using point mutants. CD44ec (positive control) and synthesized alanine-substituted peptides were immobilized on immunoplates. The plates were incubated with C<sub>44</sub>Mab-46 (1 μg/mL), followed by incubation with peroxidase-conjugated anti-mouse immunoglobulins. Optical density was measured at 655 nm. (B) Schematic illustration of the epitope recognized by C<sub>44</sub>Mab-46 using ELISA. Red aa indicate the critical epitope of C<sub>44</sub>Mab-46 determined using ELISA. aa, amino acids; IC, intracellular domain; SS, signal sequence; TM, transmembrane domain.

22.5-, and 33.8-fold decreased compared with wild type 161–180 aa, respectively, indicating that Thr174, Asp175, Asp176, Asp177, and Val178 are the binding epitope for C<sub>44</sub>Mab-46. We exhibited the ratio of the  $K_D$  values for each peptide to the  $K_D$  value for wild type p161–180 in Figure 4.

### Discussion

This study examines the C<sub>44</sub>Mab-46 epitope of CD44v3-10 by peptide scanning using ELISA and SPR. We determined the critical epitope as Asp175, Asp177, and Val178 using ELISA, and as Thr174, Asp175, Asp176, Asp177, and Val178 using SPR, which are coded in exon 5 of CD44 gene. The epitope mapping result using ELISA and SPR showed the same region of CD44v3-10 as the epitope; however, Thr174 and Asp176 are shown as the epitope only by SPR analysis. Peptides were immobilized on immunoplates in ELISA. In contrast, C<sub>44</sub>Mab-46 was immobilized on a sensor chip in SPR analysis. This difference may affect the reactivity of C<sub>44</sub>Mab-46 to these peptides.

Epitope mapping by ELISA is more rapid, and the cost of ELISA is inexpensive compared with SPR. However, it is difficult to obtain precise quantitative information of antigen–antibody interaction by ELISA, whereas SPR reveals

each interaction much more quantitatively in real time.<sup>(31)</sup> This study showed that SPR might be a more efficient method for determining the epitope residues because the intensity of the reaction of T174A and D176A to C<sub>44</sub>Mab-46 displayed almost the same value as that of wild type p161–180 to C<sub>44</sub>Mab-46 in ELISA.

In the previous study, we developed a novel epitope mapping system named RIEDL insertion for epitope mapping (REMAP) method.<sup>(32)</sup> This method is for determining the conformational epitope, which could not be determined by alanine scanning. Using the REMAP method, we determined the critical epitope of C<sub>44</sub>Mab-46 as Thr174, Asp175, Asp176, Asp177, and Val178 of CD44s, which are of the same residues with the results of this study. This is the first study indicating that the REMAP method is useful in determining the epitope compared with conventional methods such as ELISA and SPR.

Previously, we developed another anti-CD44 mAb, C<sub>44</sub>Mab-5 (IgG<sub>1</sub>, kappa),<sup>(33)</sup> whose binding epitope was determined to be 25th to 36th aa of CD44. Both anti-CD44 mAbs are used in detecting CD44s and CD44v. The epitope of C<sub>44</sub>Mab-46 is a little away from the HA-binding site, which contains Arg41, Tyr42, Arg78, Tyr79, and Arg154.<sup>(34–36)</sup> Therefore, C<sub>44</sub>Mab-46 will not block HA binding directly; however, it may affect HA

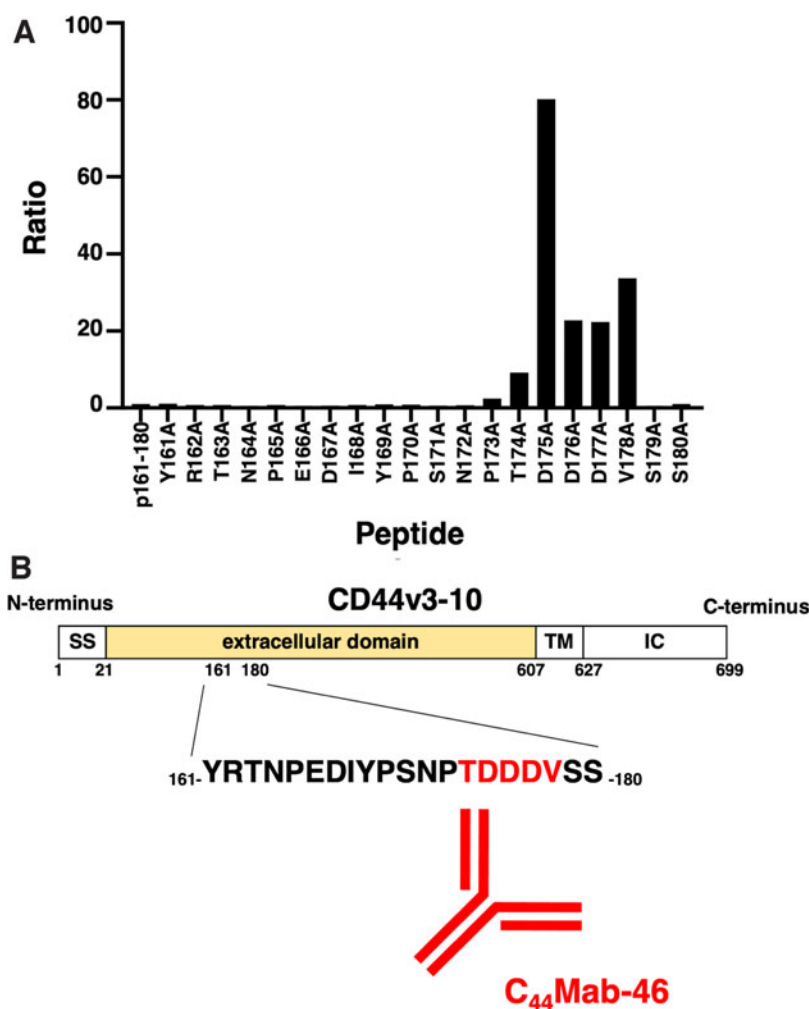


**FIG. 4.** (A) Determination of C<sub>44</sub>Mab-46 epitope of CD44v3-10 by SPR using point mutants. C<sub>44</sub>Mab-46 was immobilized on the sensor chip CM5, and peptides were injected on the sensor chip. The  $K_D$ s between C<sub>44</sub>Mab-46 and each peptide were measured using Biacore X100. The vertical axis indicates the ratio of the  $K_D$  values for each peptide to the  $K_D$  value for p161-180. (B) Schematic illustration of the epitope recognized by C<sub>44</sub>Mab-46 using SPR. Red aa indicate the critical epitope of C<sub>44</sub>Mab-46 determined using SPR. SPR, surface plasmon resonance.

binding indirectly. CD44 also has many other ligands whose binding sites have not been mapped precisely, and C<sub>44</sub>Mab-46 may affect their interaction.<sup>(15-17)</sup> Therefore, we will study the effect of C<sub>44</sub>Mab-46 on ligand binding in the future.

The subclass of C<sub>44</sub>Mab-46 is mouse IgG<sub>1</sub>, which does not have antibody-dependent cellular cytotoxicity and complement-dependent cellular cytotoxicity; therefore, we could not reveal its antitumor activity at this stage. In the previous study, we converted the IgG<sub>1</sub> subclass of C<sub>44</sub>Mab-5 into an IgG<sub>2a</sub> subclass and further produced a defucosylated version, 5-mG<sub>2a</sub>-f, and revealed its antitumor activity against mouse models of oral cancer.<sup>(37)</sup> We will convert the subclass of C<sub>44</sub>Mab-46 into IgG<sub>2a</sub> and investigate its effectiveness against CD44-expressing tumors in the future study.

#### Authors' Contributions

J.T., T.A., and H.S. performed experiments; M.K.K. designed the experiments; J.T., T.A., and Y.K. wrote the article.

#### Author Disclosure Statement

No competing financial interests exist.

#### Funding Information

This research was supported in part by Japan Agency for Medical Research and Development (AMED) under grant nos. JP21am0401013 (Y.K.) and JP21am0101078 (Y.K.), and by the Japan Society for the Promotion of Science (JSPS) Grants-in-Aid for Scientific Research (KAKENHI) grant nos. 21K15523 (to T.A.), 21K07168 (to M.K.K.), and 19K07705 (to Y.K.).

#### References

1. Ponta H, Sherman L, and Herrlich PA: CD44: From adhesion molecules to signalling regulators. *Nat Rev Mol Cell Biol* 2003;4:33-45.
2. Goodison S, Urquidí V, Tarín D: CD44 cell adhesion molecules. *Mol Pathol* 1999;52:189-196.

3. Naor D, Sionov RV, Ish-Shalom D. CD44: Structure, function and association with the malignant process. *Adv Cancer Res* 1997;71:241–319.
4. Sneath RJ, and Mangham DC: The normal structure and function of CD44 and its role in neoplasia. *Mol Pathol* 1998;51:191–200.
5. Li XP, Zhang XW, Zheng LZ, and Guo WJ: Expression of CD44 in pancreatic cancer and its significance. *Int J Clin Exp Pathol* 2015;8:6724–6731.
6. Götte M, and Yip GW: Heparanase, hyaluronan, and CD44 in cancers: A breast carcinoma perspective: Figure 1. *Cancer Res* 2006;66:10233–10237.
7. Penno MB, August JT, Baylin SB, Mabry M, Linnoila RI, Lee VS, Croteau D, Yang XL, and Rosada C: Expression of Cd44 in human lung-tumor. *Cancer Res* 1994;54:1381–1387.
8. Mayer B, Jauch KW, Gunthert U, Figdor CG, Schildberg FW, Funke I, and Johnson JP: De-novo expression of CD44 and survival in gastric cancer. *Lancet* 1993;342: 1019–1022.
9. Wielenga VJM, Heider KH, Offerhaus GJA, Adolf GR, Vandenberg FM, Ponta H, Herrlich P, and Pals ST: Expression of Cd44 variant proteins in human colorectal-cancer is related to tumor progression. *Cancer Res* 1993;53: 4754–4756.
10. Wang SJ, and Bourguignon LY: Role of hyaluronan-mediated CD44 signaling in head and neck squamous cell carcinoma progression and chemoresistance. *Am J Pathol* 2011;178:956–963.
11. Günthert U, Hofmann M, Rudy W, Reber S, Zöller M, Haußmann I, Matzku S, Wenzel A, Ponta H, and Herrlich P: A new variant of glycoprotein CD44 confers metastatic potential to rat carcinoma cells. *Cell* 1991;65:13–24.
12. Seiter S, Arch R, Reber S, Komitowski D, Hofmann M, Ponta H, Herrlich P, Matzku S, and Zöller M: Prevention of tumor metastasis formation by anti-variant CD44. *J Exp Med* 1993;177:443–455.
13. Orian-Rousseau V: CD44 is required for two consecutive steps in HGF/c-Met signaling. *Genes Dev* 2002;16:3074–3086.
14. Orian-Rousseau V: CD44, a therapeutic target for metastasizing tumours. *Eur J Cancer* 2010;46:1271–1277.
15. Wobus M, Kuns R, Wolf C, Horn LC, Kohler U, Sheyn I, Werness BA, and Sherman LS: CD44 mediates constitutive type I receptor signaling in cervical carcinoma cells. *Gynecol Oncol* 2001;83:227–234.
16. Wobus M, Rangwala R, Sheyn I, Hennigan R, Coila B, Lower EE, Yassin RS, and Sherman LS: CD44 Associates With EGFR and erbB2 in Metastasizing Mammary Carcinoma Cells. *Appl Immunohistochem Mol Morphol* 2002; 10:34–39.
17. Perez A, Neskey DM, Wen J, Pereira L, Reategui EP, Goodwin WJ, Carraway KL, and Franzmann EJ: CD44 interacts with EGFR and promotes head and neck squamous cell carcinoma initiation and progression. *Oral Oncol* 2013;49:306–313.
18. Sung H, Ferlay J, Siegel RL, Laversanne M, Soerjomataram I, Jemal A, and Bray F: Global cancer statistics 2020: GLOBOCAN estimates of incidence and mortality worldwide for 36 cancers in 185 countries. *CA Cancer J Clin* 2021;71:209–249.
19. Pai SI, and Westra WH: Molecular pathology of head and neck cancer: Implications for diagnosis, prognosis, and treatment. *Annu Rev Pathol Mech Dis* 2009;4:49–70.
20. Lee YS, Johnson DE, and Grandis JR: An update: Emerging drugs to treat squamous cell carcinomas of the head and neck. *Expert Opin Emerging Drugs* 2018;23:283–299.
21. Cramer JD, Burtneß B, and Ferris RL: Immunotherapy for head and neck cancer: Recent advances and future directions. *Oral Oncol* 2019;99:104460.
22. Wheeler DL, Huang S, Kruser TJ, Nchrebecki MM, Armstrong EA, Benavente S, Gondi V, Hsu KT, and Harari PM: Mechanisms of acquired resistance to cetuximab: role of HER (ErbB) family members. *Oncogene* 2008;27:3944–3956.
23. Widakowich C, De Castro G, De Azambuja E, Dinh P, and Awada A: Review: Side effects of approved molecular targeted therapies in solid cancers. *Oncologist* 2007;12: 1443–1455.
24. Naruse T, Yanamoto S, Okuyama K, Ohmori K, Tsuchihashi H, Furukawa K, Yamada S-I, and Umeda M: Immunohistochemical study of PD-1/PD-L1 axis expression in oral tongue squamous cell carcinomas: Effect of neoadjuvant chemotherapy on local recurrence. *Pathol Oncol Res* 2020;26:735–742.
25. Athanassiou-Papaefthymiou M, Shkeir O, Kim D, Divi V, Matossian M, Owen JH, Czerwinski MJ, Papagerakis P, McHugh J, Bradford CR, Carey TE, Wolf GT, Prince ME, and Papagerakis S: Evaluation of CD44 variant expression in oral, head and neck squamous cell carcinomas using a triple approach and its clinical significance. *Int J Immunopathol Pharmacol* 2014;27:337–349.
26. Wang SJ, Wong G, De Heer A-M, Xia W, Bourguignon LYW: CD44 variant isoforms in head and neck squamous cell carcinoma progression. *Laryngoscope* 2009;119:1518–1530.
27. Riechelmann H, Sauter A, Golze W, Hanft G, Schroen C, Hoermann K, Erhardt T, and Gronau S: Phase I trial with the CD44v6-targeting immunoconjugate bivatuzumab mertansine in head and neck squamous cell carcinoma. *Oral Oncol* 2008;44:823–829.
28. Fujii Y, Kaneko M, Neyazaki M, Nogi T, Kato Y, and Takagi J: PA tag: A versatile protein tagging system using a super high affinity antibody against a dodecapeptide derived from human podoplanin. *Protein Expr Purif* 2014;95:240–247.
29. Fujii Y, Kaneko MK, Ogasawara S, Yamada S, Yanaka M, Nakamura T, Saidoh N, Yoshida K, Honma R, and Kato Y: Development of RAP tag, a novel tagging system for protein detection and purification. *Monoclon Antib Immunodiagn Immunother* 2017;36:68–71.
30. Fujii Y, Kaneko MK, and Kato Y: MAP tag: A novel tagging system for protein purification and detection. *Monoclon Antib Immunodiagn Immunother* 2016;35:293–299.
31. Daiss JL, and Scalice ER: Epitope mapping on BIAcore: Theoretical and practical considerations. *Methods* 1994;6: 143–156.
32. Asano T, Kaneko MK, Takei J, Tateyama N, and Kato Y: Epitope mapping of the Anti-CD44 monoclonal antibody (C44Mab-46) using the REMAP method. *Monoclon Antib Immunodiagn Immunother* 2021;40:156–161.
33. Yamada S, Itai S, Nakamura T, Yanaka M, Kaneko MK, and Kato Y: Detection of high CD44 expression in oral cancers using the novel monoclonal antibody, C44Mab-5. *Biochem Biophys Rep* 2018;14:64–68.
34. Peach R, Hollenbaugh D, Stamenkovic I, and Aruffo A: Identification of hyaluronic acid binding sites in the extracellular domain of CD44. *J Cell Biol* 1993;122:257–264.
35. Liao HX, Lee DM, Levesque MC, and Haynes BF: N-terminal and central regions of the human CD44 extracellular domain

- participate in cell surface hyaluronan binding. *J Immunol* 1995; 155:3938–3945.
36. Bajorath J, Greenfield B, Munro SB, Day AJ, and Aruffo A: Identification of CD44 residues important for hyaluronan binding and delineation of the binding site. *J Biol Chem* 1998;273:338–343.
  37. Takei J, Kaneko M, Ohishi T, Hosono H, Nakamura T, Yanaka M, Sano M, Asano T, Sayama Y, Kawada M, Harada H, and Kato Y: A defucosylated anti-CD44 monoclonal antibody 5-mG2a-f exerts antitumor effects in mouse xenograft models of oral squamous cell carcinoma. *Oncol Rep* 2020;44:1949–1960.

Address correspondence to:

*Yukinari Kato*  
*Department of Antibody Drug Development*  
*Tohoku University Graduate School of Medicine*  
*2-1, Seiryō-Machi*  
*Sendai 980-8575*  
*Japan*

*E-mail: yukinarikato@med.tohoku.ac.jp*

*Received: May 27, 2021*

*Accepted: September 1, 2021*